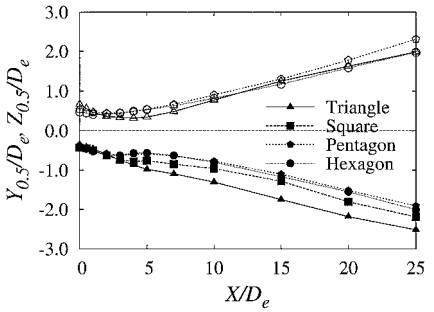

Fig. 4 Variation of half-velocity widths along vertex and side planes for polygonal jets at Mach number 1.0: solid symbols, side planes, and open symbols, vertex planes.

variation along the vertex plane in Fig. 4). Spread is maximum at locations corresponding to the midpoint of a flat side, clearly indicating the action of the large-scale structures rolling up from the flat edges. Also notice that this increased spread along the flat side direction is more pronounced in lower-order polygons. Because for polygons of equal area the length of a side of a lower-order polygon is higher than that of a higher-order polygon, it may be concluded that the length of a flat side determines the amount of spread. The area enclosed by the outermost contour ($0.1U_c$) may be taken as a measure of the size of the jet at a particular location. It is seen that the size of the lower-order polygons are larger than those of higher orders.

The half-width growths of the polygonal jets are compared in Fig. 4 for Mach number 1.0. An initial decrease in half width along the vertex planes can be seen from this plot. Observe that the hexagon, being closer to the circle, attains axisymmetry more quickly, compared to the rest of the polygons. This tendency decreases with decrease in the number of sides of the polygon. Thus, the triangular jet shows a lot of variation in its spread along vertex and side planes. The spread along side and vertex planes are different, even at 25 diameters, for triangular and pentagonal jets.

Summary

In polygonal jets, mixing processes continue to be active even in the far field. These results indicate that polygonal jets, particularly those of lower orders, may be favorably considered for use in mixing and propulsive systems.

References

[1]Koshigoe, S., Gutmark, E., Schadow, K. C., and Tubis, A., "Wave Structures in Jets of Arbitrary Shape. iii. Triangular Jets," *Physics of Fluids*, Vol. 31, No. 6, 1988, pp. 1410–1419.

[2]Quinn, W. R., "Mean Flow and Turbulence Measurements in a Triangular Turbulent Free Jet," *International Journal of Heat and Fluid Flow*, Vol. 11, No. 3, 1990, pp. 220–224.

[3]Gutmark, E., Schadow, K. C., and Wilson, K. J., "Subsonic and Supersonic Combustion Using Noncircular Injectors," *Journal of Propulsion and Power*, Vol. 7, No. 2, 1991, pp. 240–249.

[4]Van der Hegge Zijnen, B. G., "Measurements of the Velocity Distribution in a Plane Turbulent Jet of Air," *Applied Scientific Research*, Vol. A7, 1958, pp. 256–276.

[5]Marsters, G. F., "Spanwise Velocity Distributions in Jets from Rectangular Slots," *AIAA Journal*, Vol. 19, No. 2, 1981, pp. 148–152.

[6]Krothapalli, A., Hsia, Y., Baganoff, D., and Karamcheti, K., "The Role of Screech Tones in Mixing of an Underexpanded Rectangular Jet," *Journal of Sound and Vibration*, Vol. 106, No. 1, 1986, pp. 119–143.

[7]Tsuchiya, Y., Horikoshi, C., and Sato, T., "On the Spread of Rectangular Jets," *Experiments in Fluids*, Vol. 4, 1986, pp. 197–204.

[8]Tam, C. K. W., and Thies, A., "Instability of Rectangular Jets," *Journal of Fluid Mechanics*, Vol. 248, 1993, pp. 425–448.

[9]Quinn, W. R., "Streamwise Evolution of a Square Jet Cross Section," *AIAA Journal*, Vol. 30, No. 12, 1992, pp. 2852–2857.

[10]Raman, G., and Taghavi, R., "Resonant Interaction of a Linear Array of Supersonic Rectangular Jets: An Experimental Study," AIAA Paper 95-0510, 1995.

[11]Fujita, S., Osaka, H., and Ueno, G., "Three-Dimensional Jet Issuing from the Cruciform Nozzle," *Bulletin of the Japan Society of Mechanical Engineering*, Vol. 28, No. 240, 1985, pp. 1062–1068.

[12]Quinn, W. R., and Marsters, G. F., "Upstream Influence on Turbulent Jet from Cruciform Nozzles," *Aeronautical Journal*, Vol. 89, No. 882, 1985, pp. 55–58.

[13]Hussain, F., and Husain, H. S., "Elliptic Jets. Part-i: Characteristics of Unexcited and Excited Jets," *Journal of Fluid Mechanics*, Vol. 233, 1991, pp. 439–482.

[14]Gutmark, E., and Schadow, K. C., "Flow Characteristics of Orifices and Tapered Jets," *Physics of Fluids*, Vol. 30, No. 11, 1987, pp. 3448–3454.

[15]Nagai, M., "Mechanism of Pseudo-Shock Wave in Supersonic Jet," *Bulletin of the Japan Society of Mechanical Engineering*, Vol. 26, No. 212, 1983, pp. 207–214.

[16]Kline, S. J., and McClintock, F. A., "Describing Uncertainties in Single-Sample Experiments," *Mechanical Engineering*, Vol. 75, No. 1, 1953, pp. 3–8.

[17]Quinn, W. R., "On Mixing in an Elliptic Turbulent Free Jet," *Physics of Fluids A*, Vol. 1, No. 10, 1989, pp. 1716–1722.

P. J. Morris
Associate Editor

Marching Distance Functions for Smooth Control of Hyperbolic Grids

Gökhan Durmuş* and Mehmet Şerif Kavsaoğlu†
Middle East Technical University, 06531 Ankara, Turkey

Nomenclature

C	= airfoil chord length
CSI	= grid control parameter in ξ direction: when <1, clustering; when >1, rarefying
c	= grid point chord length
i, j	= grid indices, related to ξ and η directions, respectively
$\boldsymbol{i}$, $\boldsymbol{j}$	= unit vectors along x and y directions
i_ξ	= i level to be controlled for grid control in ξ direction
J	= Jacobian
j_η	= j level to be controlled for grid control in η direction
j_ξ	= j level to be controlled for grid control in ξ direction
$\boldsymbol{r}$	= position vector
s	= grid spacing in η direction; marching distance
s_{j_η}	= specified value of the marching distance at j_η for grid control in η direction
s_1	= initial grid spacing in η direction from the surface
s^s	= exponential grid spacing function, for grid control in η direction from the surface
s^η	= grid spacing function for grid control in η direction at a specified j level
V	= cell volume or inverse Jacobian
x, y	= Cartesian coordinates
Δi_ξ	= interval of i levels for grid control in ξ direction
Δj_η	= interval of j levels for grid control in η direction
Δj_ξ	= interval of j levels for grid control in ξ direction
ε, ε^*	= grid control parameter in η direction; ratio of the change in grid spacing to grid spacing in η direction, $\Delta s/s$
ξ, η	= curvilinear coordinates

Introduction

THE hyperbolic grid generation methods have the advantages of good orthogonality, ease of clustering, and efficiency in computation time. Their fundamental principles and recent developments

Received 9 March 1999; revision received 16 November 1999; accepted for publication 21 June 2000.

*Graduate Student, Department of Aeronautical Engineering; also Research Assistant, Anadolu University Civil Aviation School, 26470 Eskişehir, Turkey.

†Associate Professor, Department of Aeronautical Engineering. Senior Member AIAA.

are available in the literature.[1–3] In general, the clustering is applied at the surface and in the η direction, which is normal to the surface. Here, a new method is presented that makes it possible to cluster or rarefy the grid lines smoothly in the ξ and/or η directions at arbitrary locations. The hyperbolic equations are obtained by the orthogonality condition and the cell volume specification. In the two-dimensional space, they are given as

$$\boldsymbol{r}_\xi \cdot \boldsymbol{r}_\eta = x_\xi x_\eta + y_\xi y_\eta = 0$$

$$\boldsymbol{r}_\xi \times \boldsymbol{r}_\eta = x_\xi y_\eta - x_\eta y_\xi = V = J^{-1} \tag{1}$$

These equations are solved by marching in the η direction. The local cell volume is defined as

$$V_{i,j} = c_{i,j} s_{i,j} \tag{2}$$

The grid point chord length c_{ij} is given by

$$c_{i,j} = \tfrac{1}{2}(|\boldsymbol{r}_{i,j} - \boldsymbol{r}_{i-1,j}| + |\boldsymbol{r}_{i+1,j} - \boldsymbol{r}_{i,j}|) \tag{3}$$

The marching distance s_{ij} can be expressed as a function for the grid control. In the present work, the derivative expressions of the linearized hyperbolic equations are approximated by the second-order central differences in the ξ direction and by the first-order backward differences in the η direction. Artificial dissipation terms are added to control the oscillations and the smoothness.[2]

Grid Control

A. Grid Control in η Direction from Surface

One of the ways of controlling the grids at the surface is to use an exponential function for the marching distance[2] $s^s(j)$:

$$s^s(j) = s_1(1+\varepsilon)^{j-1} \tag{4}$$

where s_1 and ε are the required parameters. The local marching distance is given by

$$s(i, j) = s^s(j) \tag{5}$$

B. Grid Control in η Direction at a Specified j Level

The interior grids may be controlled by the same method. An exponential function can also be used as a control tool. The value of the grid control parameter is recalculated and renamed ε^* at the interval of control (Δj_η in Fig. 1) as

$$\varepsilon^* = \left[\frac{s^s(j_\eta - \Delta j_\eta/2)}{s_{j_\eta}}\right]^{2/\Delta j_\eta} - 1 \tag{6}$$

where

$$s^s(j_\eta - \Delta j_\eta/2) = s_1(1+\varepsilon)^{(j_\eta - \Delta j_\eta/2 - 1)} \tag{7}$$

and the marching function is redefined as

$$s^\eta(j) = \begin{cases} s_{j_\eta}(1+\varepsilon^*)^{j_\eta - j} & \text{for} \quad j_\eta - \Delta j_\eta/2 \le j \le j_\eta \\ s_{j_\eta}(1+\varepsilon^*)^{j - j_\eta} & \text{for} \quad j_\eta \le j \le j_\eta + \Delta j_\eta/2 \end{cases} \tag{8}$$

and gives controllability in the η direction over the entire perimeter of the grid. In Fig. 1, both the surface clustering and the additional clustering in η is shown. There is a nonsmooth connection, which does not significantly affect the grid quality. It could also be changed with a smooth one. For the interval of control, the local marching distance is obtained from

$$s(i, j) = s^\eta(j) \tag{9}$$

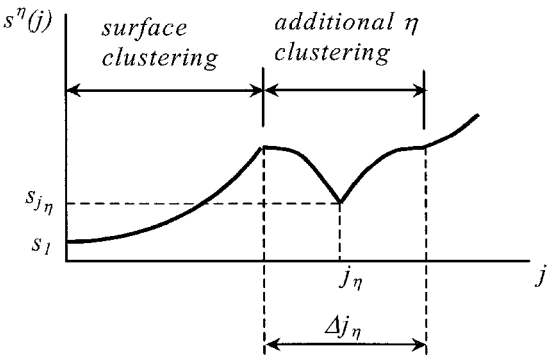

Fig. 1 Variation of marching distance function s^η along η direction.

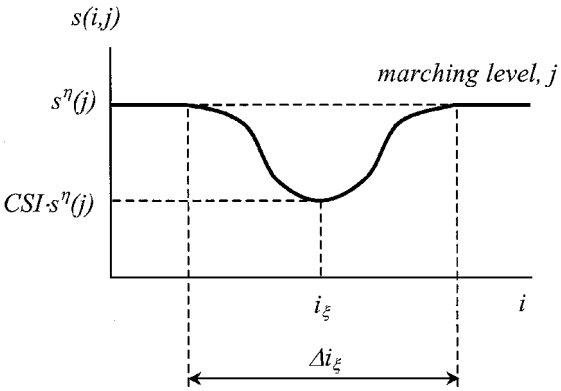

Fig. 2 Variation of marching distance $s(i, j)$ along ξ direction.

C. Grid Control in ξ Direction at a Specified i, j Level

The grid control in the ξ direction is obtained in a similar fashion. A gradual variation of the marching distance, along the ξ direction, indirectly affects the grid point chord length distribution of the next η level. A smoother and more parametric function is needed for the marching distance. Because it uses only a portion of the marching level, any discontinuity at that level affects the quality of the overall grid. A sinusoidal function may be a good choice for clustering, as shown in Fig. 2. In this case, the local marching distance will be calculated from the following:

$$s(i, j) = 0.5 s^\eta(j)\left[1 + CSI + CS\cos\left(\pi \frac{i - i_\xi + \Delta i_\xi/2}{\Delta i_\xi/2}\right)\right] \tag{10}$$

for the specified intervals of control

$$j_\xi - \Delta j_\xi/2 \le j \le j_\xi + \Delta j_\xi/2$$

$$i_\xi - \Delta i_\xi/2 \le i \le i_\xi + \Delta i_\xi/2$$

where

$$CS = (1 - CSI)\sin\left(\pi \frac{j - j_\xi + \Delta j_\xi/2}{\Delta j_\xi}\right) \tag{11}$$

for

$$i_\xi - \Delta i_\xi/4 \le i \le i_\xi + \Delta i_\xi/4$$

and

$$CS = (1 - CSI) \tag{12}$$

for

$$i_\xi - \Delta i_\xi/2 \le i < i_\xi - \Delta i_\xi/4$$

$$i_\xi + \Delta i_\xi/4 < i \le i_\xi + \Delta i_\xi/2$$

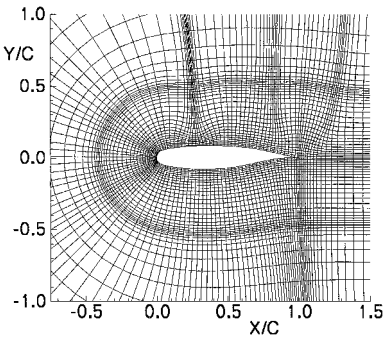

Fig. 3 Sample grid around NLR-7301 airfoil.

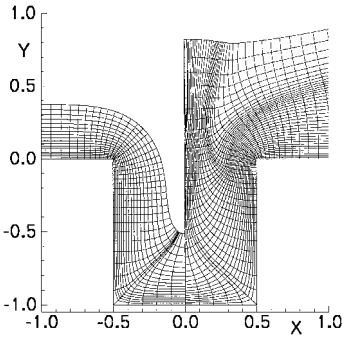

Fig. 4 Comparison of two grids generated around a cavity without ($X < 0.0$) and with ($X > 0.0$) using the present marching distance functions.

Results

To present the new method developed here, a sample grid was generated around the National Aerospace Laboratory- (NLR-) 7301 airfoil as shown in Fig. 3. For this grid, the surface clustering was applied by using $s_1/C = 0.01$ and $\varepsilon = 0.1$. The applications of the grid control for the interior domain are also presented. In Fig. 3, the additionally clustered lines in the η direction, the clustered lines in the ξ direction above the front-half of the airfoil, and the rarefied lines in the ξ direction above the trailing edge can all be easily observed.

In Fig. 4, two grids developed around a cavity are compared. The grid at the left side of the symmetry line ($X = 0.0$) was obtained without using the marching distance functions. For this grid, grid lines crossed after the 19th η level. The grid at the right side of the symmetry line was produced by using multiple controls in the ξ direction. The grid line crossings were eliminated, and a controlled interior point distribution was obtained. For both grids, all of the other parameters were exactly the same. For these cavity cases, some local imperfections were removed by applying a simple algebraic smoothing procedure after completion of the hyperbolic grids.

Conclusions

The marching distance functions, as presented here, can be used when there is a need for interior domain grid control, such as in problems with shocks or in problems with cavities where the generation of grids is relatively more difficult. They can also be useful for the solution adaptive grid generation procedures.

References

[1]Chan, W. M., "Hyperbolic Methods for Surface and Field Grid Generation," *Handbook of Grid Generation*, edited by J. F. Thompson, B. K. Soni, and N. P. Weatherill, CRC Press, Boca Raton, FL, 1999, pp. 5.1–5.26.

[2]Chan, W. M., and Steger, J. L., "Enhancements of a Three-Dimensional Hyperbolic Grid Generation Scheme," *Applied Mathematics and Computation*, Vol. 51, No. 1, 1992, pp. 181–205.

[3]Tai, C. H., Chiang, D. C., and Su, Y. P., "Three Dimensional Hyperbolic Grid Generation with Inherent Dissipation and Laplacian Smoothing," *AIAA Journal*, Vol. 34, No. 9, 1996, pp. 1801–1806.

P. Givi
Associate Editor

Ignition Mechanisms of Jet-A Fuel Vapor in a Confined Environment

Tae-Woo Lee*
Arizona State University, Tempe, Arizona 85287-6106

Introduction

IGNITION mechanisms of jet-A fuel vapor are of interest for safety reasons during storage in aircraft fuel tanks. Fuel vapor is present in the ullage (air space above the remaining fuel) of all fuel tanks. Fuel vapor can accumulate in fuel tanks as fuel consumption increases the empty volume in the tank. Under certain flight and ground conditions, the fuel vapor mixed with the available air in the tank is within flammable limits. Some recent work has been done by Shepherd et al.,[1] but current data on ignition characteristics of jet fuels are far from complete. In addition, the ignition mechanisms in confined environments with realistic probability of occurrence need to be identified correctly and eliminated.

The necessity to obtain data on ignition mechanisms and so-called minimum ignition energy of jet-A fuel vapor has recently been reemphasized due to the highly publicized incident involving TWA flight 800. Whereas the frequency of such an incident is very small, these events are unpredictable and catastrophic in nature. Also, any measure that is taken to minimize an ignition event in aircraft fuel tanks should be based on quantitative data on jet-A fuel vapor flammability, as well as on an understanding of the origin of these ignition events.

Ignition is a much explored area in combustion science, and numerous studies have been devoted to characterizing ignition of gas- and liquid-phase fuels (see Refs. 2–7 as examples). However, studies of jet-A fuel vapor for applications in fuel tank safety have been relatively few, uncorrelated with one another, and at times with insufficiently defined test conditions. Only in the recent past have more careful reports summarizing jet-A fuel vapor flammability been published.[1,8] Both the reports by Hill[8] and Shepherd et al.[1] include a review of the previous historical measurements[9–11] of jet-A fuel vapor flammability limits. Some of the factors that make the use of the previous data on jet-A fuel vapor flammability difficult are 1) undefined fuel batch flashpoint or other fuel characteristics, 2) variations in the criterion for fuel vapor ignition, 3) variations in the electrode configurations and spark deposition modes (spark duration, etc.), 4) differences in the test chamber scale/geometry and, therefore, fuel thermal conditions, and 5) undefined fuel loading or variations thereof.

Recent data reported by Shepherd et al.[1] and Naegeli and Childress[12] offer more information on the jet-A fuel vapor ignition limits under well-defined conditions. However, because the focus of the report by Shepherd et al.[1] was on determination of the cause of the TWA 800 accident, it did not necessarily include a coverage of conditions generally applicable for all of the phases of a flight. The work by Naegeli and Childress[12] mostly involves a comparison of different jet fuels and correlation with their chemical contents.

Here, we report on ignition limits of jet-A fuel vapor as a function of the fuel loading using conventional electrical sparks. In addition, we present a much more relevant ignition mechanism for accidental ignition events involving electrical contact sparks and demonstrate its capability to ignite fuel–air mixtures at very low voltage and power settings.

Experimental Methods

Combustion Chamber

The combustion chamber consisted of a three-port, stainless-steel chamber for atmospheric to vacuum operations. The chamber had

Received 15 February 2000; revision received 11 June 2000; accepted for publication 12 June 2000.

*Associate Professor, Department of Mechanical and Aerospace Engineering.